Integration of Full-scale Test, Laboratory Characterization, and Finite Element Modeling for Reflective Cracking in Airport Pavements

Tirupan Mandal[1], Hao Yin[1], Richard Ji[2], and Ryan Rutter[2]
([1] Gemini Technologies, Inc., 3153 Fire Rd, Egg Harbor Township, NJ 08234, USA, email: tirupan.mandal@gemitek.com, hao.yin@gemitek.com)
([2] Federal Aviation Administration, Airport Technology R&D Branch, William J. Hughes Technical Center, Atlantic City International Airport, NJ 08234, USA, email: richard.ji@faa.gov, ryan.rutter@faa.gov)

ABSTRACT

In airfields, the potential for reflective cracking presents a major challenge for rigid pavement rehabilitation involving asphalt overlays. The change in temperature in the pavement causes the contraction and expansion in the underlying concrete slabs, thus resulting in reflective cracking. The traffic loading further aggravates these thermally-induced cracks. In this study, a customized Overlay Tester (OT) was used in the laboratory to simulate the full-scale test conditions. Tests were run on field extracted hot mix asphalt (HMA) cores. The laboratory testing also evaluated three types of cooling effects – control, high, and extreme – on the initiation and propagation of reflection cracks on the above-mentioned HMA cores. Various reflective cracking parameters (strain, fracture, and fatigue) were found to characterize between the different cooling sets successfully. Initial strain parameter was found to correlate well with full-scale test data (R^2 = 0.97). Three regression models were also developed to estimate the reflective cracking parameters (fatigue parameters and critical fracture energy) using a finite element model.

Keywords: Reflective cracking, Overlay Tester, Fracture energy, Failure Strain, FEM

1. INTRODUCTION

Reflective cracking is one of the main distresses found in asphalt overlays which can occur in overlays placed on rigid pavements, overlays on cracked asphalt pavements, and even asphalt layers with cement-treated base pavements. Series of full-scale experiments have been conducted at the Federal Aviation Administration (FAA) National Airport Pavement Test Facility (NAPTF) to study reflective cracking for airfields [1-4]. In the laboratory, Texas Overlay Tester (OT) [5] has been used by many researchers [6-10, 22-26] to study reflective cracking as it simulates the horizontal joint movements in the joint/crack vicinity of PCC pavements. The OT has also been customized to simulate the full-scale testing at the NAPTF [11]. The objectives of this paper were:

- Evaluate different cooling effects on the performance of hot mix asphalt (HMA) mixtures using the customized OT.
- Correlate laboratory test results to full-scale tests.
- Develop a finite element model to predict reflective cracking parameters.

2. TEST METHODS

2.1 Full-scale Testing

Figure 1(a) shows the full-scale test overlay at the FAA NAPTF which consisted of two 1.5-m wide HMA overlay strips atop two 0.31-m. thick, 4.6- by 4.6-m concrete slabs. Both strips had the same materials, FAA P-401 Performance Grade 64-22 (PG 64-22) HMA. Crack initiation and propagation were monitored through instrumentation sensors. During the overlay construction, H-type asphalt strain gages (EG) were installed at the bottom of each lift. Further, surface strain gages (SG) were installed at the various locations on the pavement surface and edges (Figure 1(b)) after the pavement temperature stabilized.

(a) Overlay Pavement (b) Crack through Strain Gage

FIGURE 1 Full-scale Testing at FAA NAFTF

Full-scale tests were operated using the Temperature Effect Simulation System (TESS), which consisted of hydraulic and temperature units. The temperature unit was designed to maintain the overlay bottom temperature at 0° C, which was identified as the critical temperature [12]. Daily temperature variations were approximated by a haversine waveform describing the relationship between the joint opening and cycle time as shown in Eq.(1):

$$d(t) = D\sin^2\left(\frac{\pi}{2} + \frac{\pi t}{T}\right) + R \qquad \text{Eq.(1)}$$

where t is the time of interest, D is the amplitude of joint opening, T is the cycle time, and R is rest period, which was included at the end of each loading cycle to allow the HMA materials to relax.

2.2 Customized Overlay Tester

To study the temperature effects on the initiation and propagation of HMA mixtures, the laboratory testing program included three sets. In the first set (Control set), a displacement rate of 0.004 mm/sec was used, which simulated the full-scale experiment. In the second set (Cooling set), a higher displacement rate of 0.008 mm/sec was used to represent a sudden cooling event. In the last set (Extreme set), a mixed displacement rate of the first two sets was used. Assuming extreme cooling occurs in 30 days of a typical year, for every 12 loading cycles, there would be 11 cycles of 0.004 mm/sec and 1 cycle of 0.008 mm/sec. The tests were conducted at a temperature of 0° C and a rest period of 150 s was applied after each cycle for each set. Figures 2(a) and 2(b) show the specimen instrumentation of the customized OT and the test specimen (with SGs attached), respectively.

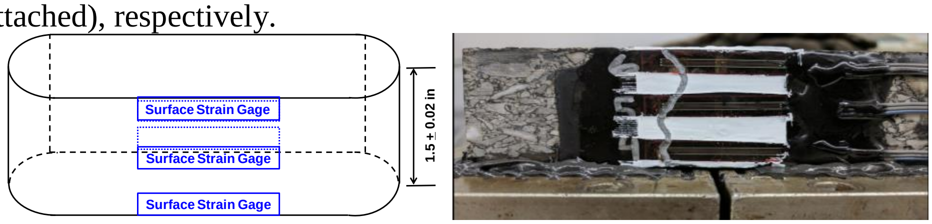

(a) Specimen Instrumentation (b) Test Specimen

FIGURE 2 Customized OT Specimen Instrumentation

2.3 Finite Element Modeling

Parallel to laboratory testing, finite element modeling (FEM) was conducted using the software ABAQUS to simulate the OT test. Some of the material input properties are shown in Table 1 with reference to literature next to them (in square brackets). The thermal properties were assumed on the basis of the works of literature [13-20]. A hex-structured mesh was used and the region was modeled using the 8-node coupled temperature displacements, C3D8RHT reduced integration elements. In the finite element analysis (FEA), two coupled temp-displacement analysis steps were constructed (including the viscoelastic behavior), one for loading and the second for the rest period. The finite element model was subjected to a constant temperature of 0° C as done in the customized OT.

TABLE 1 FEM Material Properties

Material Properties	HMA Specimen	Steel Plates
Young's Modulus (GPa)	Relaxation modulus at infinite time	200 [13,14]
Poisson's Ratio	0.35 [13,14]	0.3 [13,14]
Unit weight (kg/m^3)	2300 [13-15]	8050 [13]

Viscoelastic Properties for HMA Specimen (Ref. Temperature: 0° C, c1=18.7, c2=143.6)											
gi	0.107	0.036	0.153	0.163	0.215	0.156	0.096	0.035	0.019	0.002	0.007
τi	2E-5	2E-4	2E-3	2E-2	2E-1	2	2E+1	2E+2	2E+3	2E+4	2E+5

3. RESULTS AND ANALYSIS

3.1 Customized Overlay Tester

Customized OT tests were conducted at a temperature of 0° C with at least 5 replicates for each set. Because the number of cycles to failure ($N_{f(final)}$) has been found extremely variable [5, 21]; the test data was analysed using the "normalized load x cycle" (NLC) method [7]. The NLC method was used to identify the failure point of each specimen, which is defined as the transition from micro-crack to macro-crack propagation [7]. Accordingly, three fatigue parameters were determined: 1) $N_{f(NLC)}$: represented the number of cycles to the failure point, 2) $N_{f(crack)}$: the load value was usually found to decrease at a higher rate after the $N_{f(NLC)}$ failure point; the number of cycles to reach this point was denoted as $N_{f(crack)}$, and 3) $N_{f(czone)}$, which denoted the number of cycles between $N_{f(crack)}$ and $N_{f(NLC)}$, in other words, $N_{f(czone)}$ indicated the zone where the micro cracks start to appear to full initiation of the crack. Figure 3(a) shows the determination of the failure point for one of the specimens in the Control set, while, Figure 3(b) illustrates a representative graph of the fatigue parameters from the same specimen. Full-scale test data is also plotted in the same figure for comparison purpose, highlighting the different fatigue parameters ($N_{f(NLC)}$, $N_{f(crack)}$, and $N_{f(czone)}$) determined from the NLC method.

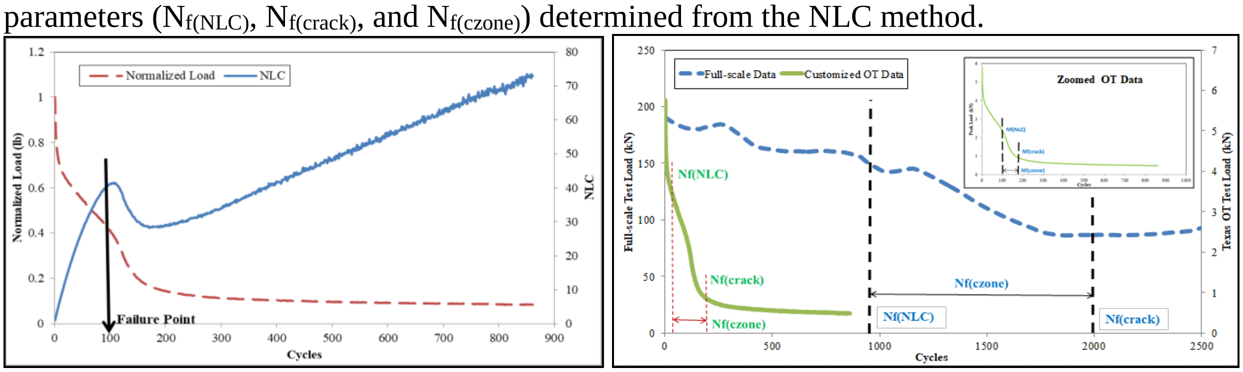

(a) Determination of Failure Point **(b) Fatigue Parameters**

FIGURE 3 Customized OT Analysis Using NLC Method

As the Extreme set is the worst condition among the three sets, the fatigue parameters for that set was found the lowest (Figure 4(a)). The values for $N_{f(czone)}$ were found to be consistent – Control Set > Cooling Set > Extreme Set, as the displacement rate of the control set was the lowest between the three sets. The Control set was higher by ~23% and ~40% than the Cooling set and Extreme set, respectively. The error bars in Figure 4(a) represent the standard deviation between the replicates. Similar high variation in the results was also reported by Ma[7].

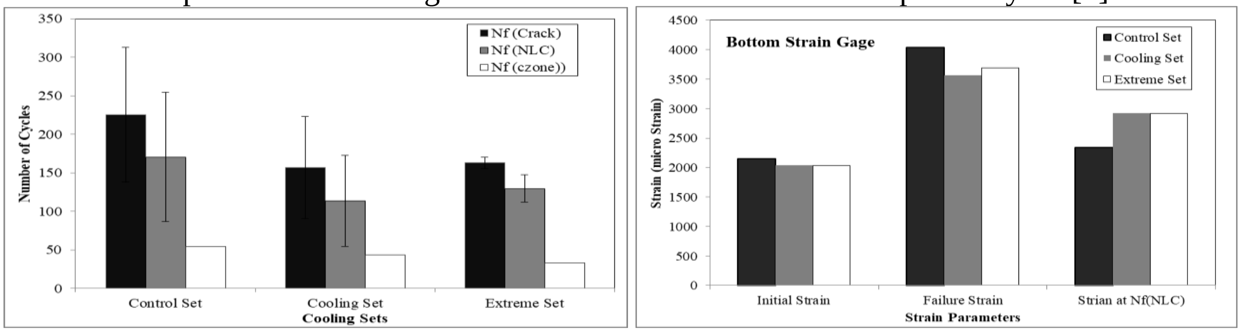

(a) Fatigue Parameters **(b) Strain Parameters**

FIGURE 4 Data Analysis for Customized OT

Further data analysis was done using the data from the strain gages (SG). Following previous analyses [11], three parameters were determined: 1) initial strain, which is the peak strain for the first cycle, 2) failure strain, which is the strain at inflection point (IF) (IF is defined as the point where the response curve undergoes a sudden change during continued loading), and 3) strain at $N_{f(NLC)}$, which is defined as the strain calculated at the failure point. Figure 4(b) shows the average values of these strains at bottom SG locations. A similar trend was seen for middle and top SG locations. Among the three strain parameters, the initial strain was lowest and failure strain was highest for all the gage locations as excepted. Between the three cooling sets, the values for initial strain and failure strain were higher for the Control set than Cooling set, and the Extreme set was found to be the lowest. This is likely due to the fact that Control set had the lowest displacement rate and thus took more loading cycles to initiate the crack; the Extreme set was the mix of Control and Cooling sets, which made the crack initiation sooner than the other two sets. In general, the average values for all replicates for both initial strain and failure strain at the bottom gage had ~5%-12% higher values for the Control set when compared to the Cooling and the Extreme sets. The strain values at $N_{f(NLC)}$ was also seen to somewhat distinguish the three sets and the gage locations as well. Critical fracture energy (G_c) as described by Garcia et al. [6] was also calculated for each set. The average value for the control set was found to have highest G_c (336 J/m^2) as compared to Cooling (321 J/m^2) and Extreme sets (297 J/m^2).

3.2 Correlation between Full-scale Test and Customized OT

The HMA overlay in the full-scale test was completely separated after 3757 loading cycles with a load reduction of 79% at the end of the test [4]. The overlay failure occurred around 2500 cycles. Initial strain parameter, which distinguished the three cooling sets, was used to correlate the full-scale and the Control set of customized OT test results. A good correlation (R^2 = 0.97) as shown in Figure 5 was found, indicating that the laboratory measured strain values were about 2.5 times the full-scale data. For fatigue parameters ($N_{f(NLC)}$, $N_{f(crack)}$, $N_{f(czone)}$), shift factors (which is the ratio of laboratory testing value to full-scale testing value) were found to be 0.2, 0.1, and 0.05, respectively.

3.3 Finite Element Analysis

Figure 6(a) shows the meshed OT model constructed in ABAQUS, which consisted of the HMA specimen and two steel plates. Similar to the customized OT test, the bottom nodes of the left plate were restricted from translation while a prescribed ramp motion was applied to the right steel plate. Only the first loading cycle of the Control and Cooling sets was simulated and analysis results are presented here.

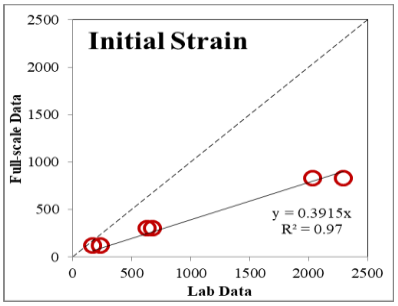

FIGURE 5 Comparison between Full-scale and Customized OT (Control Set) Data

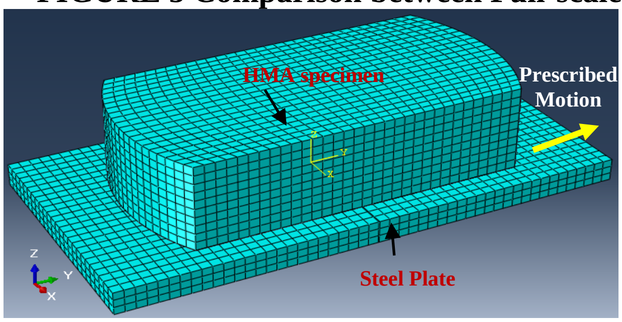

(a) Meshed FEM Model

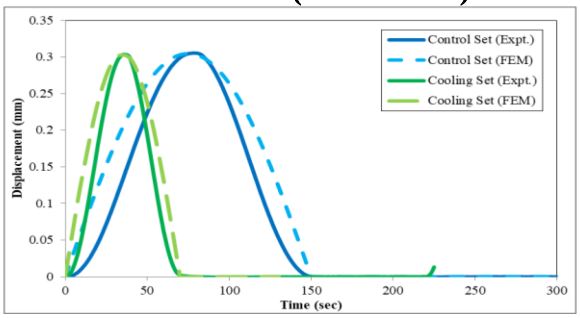

(b) Displacement Comparisons

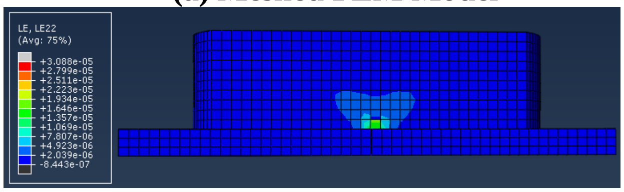

(c) Strain contour at 30 seconds

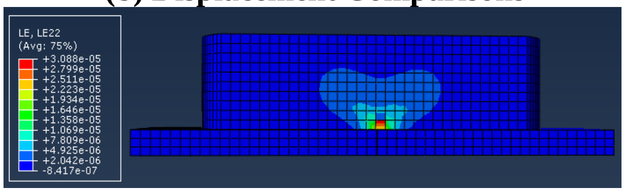

(d) Strain contour at 75 seconds

FIGURE 6 FEM Model Analysis

A reasonable agreement between the simulated displacements of the FEM and measured values from the OT was observed (Figure 6(b)). A similar observation was also noted by Ramos et al. [14]. Initial strains computed from the FEM model at the bottom of the HMA mixture were found to follow the same trend as the experimental results (Table 2). Figure 6(c) and 6(d) shows an example for the strain contour for the Control sets at two different times (30- and 75-s). It's clear that the damage zone initiated at the bottom of HMA specimen and continued to grow as the loading time increased. Using the data from the Control set, Cooling set, and full-scale testing, a regression function was developed to predict fatigue parameters ($N_{f(NLC)}$ and $N_{f(crack)}$) (Figure 7(a)). The relationships between these fatigue parameters and initial strain are expressed in Eq.(2) and Eq.(3).

$$N_{f(NLC)} = a_1 \times IS_b^{-b_1} \quad \text{Eq.(2)}$$

$$N_{f(crack)} = a_2 \times IS_b^{-b_2} \quad \text{Eq.(3)}$$

where $N_{f(NLC)}$ and $N_{f(crack)}$ are fatigue parameters, IS_b is the initial strain at bottom of specimen and a_1, a_2, b_1, and b_2 are model coefficients. In this study the values of a_1, a_2, b_1, and b_2 were found to be 4e11, 8e11, 2.859, and 2.894, respectively.

TABLE 2 Strain Comparison between Experimental and FEM study

Set	Initial Strain (Bottom) (microstrains)	
	Experimental Data	FEM Data
Control	2146.8	2697
Cooling	2042.8	2346

Further, when the fatigue parameters are determined from these models, the critical fracture energy (determined from the first cycle in OT [6]) can be approximated from Eq.(4).

$$G_c = \frac{k_1 \times N_{f\,(NLC)}}{N_{f\,(crack)} - k_2} \qquad \text{Eq.(4)}$$

where $N_{f(crack)}$ and $N_{f(NLC)}$ are fatigue parameters, G_c is the critical fracture energy (J/m^2), and k_1 and k_2 are model coefficients. For this study, k_1 and k_2 were calculated as 335.8 and 62.4, respectively. This concept when plotted for the Control set, Cooling set, and full-scale testing had a good to correlation ($R^2 = 0.82$). The correlation for just the laboratory specimens (Control and Cooling sets) had a better fit ($R^2 = 0.98$) as seen in Figure 7(b) ($R^2 = 0.74$ if the outlier is removed [circled]).

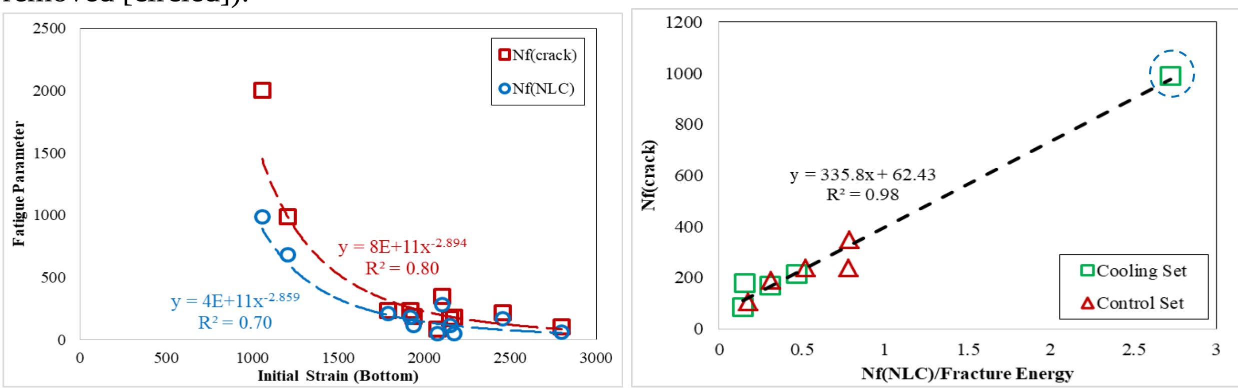

(a) Model for Fatigue Parameters **(b) Model for Fracture Energy**

FIGURE 7 Regression Models

Figure 8 shows the significance of the FEA where the OT parameters can be estimated from dynamic modulus data of the known HMA mixture. Dynamic modulus test is a very common and easy test ran on asphalt mixtures as compared to customized OT (due to testing time and specimen fabrication). Hence, using FEA to evaluate OT parameters is beneficial for future reflective cracking research.

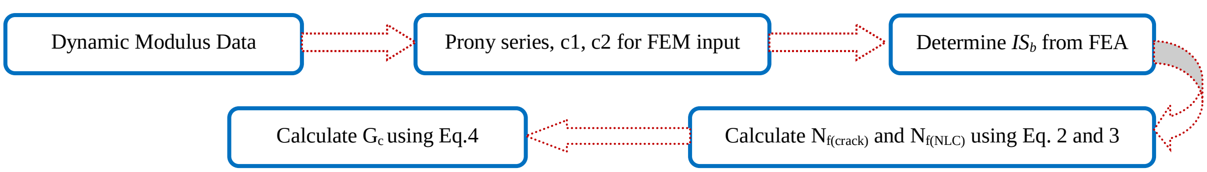

FIGURE 8 Flow Chart for using Dynamic Modulus and FEM/A to Predict customized OT Parameters

4. CONCLUSIONS

- The customized OT successfully evaluated the different cooling effects using strain parameters (initial strain, failure strain, and strain at $N_{f(NFC)}$), fatigue parameters ($N_{f(NLC)}$, $N_{f(crack)}$, and $N_{f(czone)}$), and fracture properties. The Control set mimicked the same conditions as the full-scale testing and the initial strain parameter was found to correlate well ($R^2 = 0.97$) between the two tests. A set of shift factors for fatigue parameters were also derived.
- FEM was utilized to simulate the customized OT and a good match between the calculated and measured values was observed. Through the limited experimental dataset, a conceptual approach using FEM and empirical functions (regression models) to characterize reflective cracking for airport pavements is proposed.

5. REFERENCES

[1] Yin H. Reflective Cracking Phase I Comprehensive Report, FAA Report, 2016.

[2] Yin H. Reflective Cracking Phase II Comprehensive Report, FAA Report, 2017.

[3] Yin H. Reflective Cracking Phase III Comprehensive Report, FAA Report, 2017.

[4] Yin H. Reflective Cracking Phase IV Comprehensive Report, FAA Report, 2017.

[5] TxDOT Tex-248-F: Test Procedure for Overlay Test, Texas Department of Transportation Standard, 2014.

[6] Garcia V, Miramontes A, Garibay J, Abdallah I, and Nazarian S. Improved Overlay Tester for Fatigue Cracking Resistance of Asphalt Mixtures, TxDOT 0-6815-1, 2017.

[7] Ma W. Proposed Improvements to Overlay Test for Determining Cracking Resistance of Asphalt Mixtures, MS Thesis, Auburn University, USA, 2014.

[8] Walubita F, Das G, Espinoza E, Oh J, Scullion T, Nazarian S, Abdallah I, and Garibay L. Texas Flexible Pavements and Overlays: Data Analysis Plans and Reporting Format, FHWA/TX-11/0-6658-P3, 2012.

[9] Zhou F and Scullion T. Upgraded OT and its application to characterize reflection cracking resistance of asphalt mixtures, FHWA/TX-04/0-4467-1, 2003.

[10] Zhou F and Scullion T. Overlay Tester: A Rapid Performance Related Crack Resistance Test, FHWA/TX-05/0-4467-2, 2005.

[11] Mandal T, Yin H, Ji R, and Rutter R. Laboratory Simulation of Extreme Cooling Effects on the Propagation of Reflection Cracks using Customized Texas Overlay Tester, International Conference on Highway Pavements and Airfield Technology, Philadelphia, Pennsylvania, USA, pp. 81-93, 2017.

[12] Yin H and Barbagallo D. Development of Full-scale Reflective Cracking Test at FAA NAPTF, Transportation Research Record No.2368, 2013.

[13] Qadir A and Guler M. Finite Element Modeling of Thermal Stress Restrained Specimen Test, 5th Eurasphalt & Eurobitume Congress, Istanbul, 2012.

[14] Ramos E, Gutierrez A, Tirado C, Stewart C, Abdallah I, and Nazarian S. Explaining Overlay Tester Results with Digital Image Correlation and Finite Element Analysis, International Conference on Transportation and Development, 884-894, 2016.

[15] Mandal T. Enhancement of the Asphalt Thermal Cracking Analyser (ATCA) Test to Allow Measuring Critical Properties Affecting Cracking of Asphalt Mixtures, PhD Thesis, University of Wisconsin-Madison, 2016.

[16] Cho W, Kwon S, and Choi J. The thermal conductivity for granite with various water contents, Engineering Geology, Vol. 107, No. 3-4, pp. 167-171, 2009.

[17] Monachos. Conductivity table for various materials, [Online]. Available: http://www.monachos.gr/en/resources/Thermo/conductivity.asp. [Last accessed 9-14-2017].

[18] Elert G. Conduction [Online]. Available: http://physics.info/conduction/. [Last accessed 9-17-2017]

[19] Atkins N. Specific Heats of Various Substances, Lyndon State Collage [Online]. Available: http://apollo.lsc.vsc.edu/classes/met130/notes/chapter2/spec_heats.html. [Last accessed 9-14-2017].

[20] Georgia State University. Specific heats and molar heat capacities for various substances at 20 C, [Online]. Available: http://hyperphysics.phy-astr.gsu.edu/hbase/tables/sphtt.html. [Last accessed 9-14-2017].

[21] Walubita LF, Faruk AN, Koohi Y, Luo R, Scullion T, and Lytton RL. The Overlay Tester: Comparison with Other Crack Test Methods and Recommendations for Surrogate Crack Tests, FHWA/TX-13/0-6607-2, 2013.

[22] Zhou F, Hu S, and Scullion T. Development and Verification of the Overlay Tester based Fatigure Cracking Prediction Approach, FHWA/TX-07/9-1502-01-8, 2007.

[23] Dave EV, Ahmed S, and Buttlar WG. Laboratory and Computational Evaluation of Compact Tension Fracture Test and Texas Overlay Tester for Asphalt Concrete, 7th RILEM International Conference on Cracking in Pavements, pp. 409–418, 2012.

[24] Zhou F, Chen D, Scullion T, and Williammee R. Overlay Tester: A Simple Test to Evaluate the Reflective Crackign Resistance of Asphalt Mixtures, 5th RILEM International Conference on Reflective Cracking in Pavements, 597-604, 2004.

[25] Walubita LF, Das G, Espinoza E, Oh J, Scullion T, Nazarian S, Abdallah I, and Garibay JL. Texas Flexible Pavements and Overlays: Data Analysis Plans and Reporting Format, FHWA/TX-11/0-6658-P3, 2012.

[26] Walubita LF, Faruk AN, Koohi Y, Luo R, Scullion T, and Lytton RL. The Overlay Tester (OT): Comparison with other crack test methods and recommendations for surrogate crack tests, FHWA/TX-13/0-6607-2, 2013.